



**Providing Choice & Value**

Generic CT and MRI Contrast Agents



**FRESENIUS  
KABI**

**CONTACT REP**

**AJNR**

**Pyogenic Brain Abscess: Findings from *In Vivo* 1.5-T and 11.7-T *In Vitro* Proton MR Spectroscopy**

Ping H. Lai, Kun T. Li, Shu S. Hsu, Chia C. Hsiao, Chi W. Yip, S. Ding, Lee R. Yeh and Huay B. Pan

This information is current as  
of July 16, 2025.

*AJNR Am J Neuroradiol* 2005, 26 (2) 279-288  
<http://www.ajnr.org/content/26/2/279>

# Pyogenic Brain Abscess: Findings from *In Vivo* 1.5-T and 11.7-T *In Vitro* Proton MR Spectroscopy

Ping H. Lai, Kun T. Li, Shu S. Hsu, Chia C. Hsiao, Chi W. Yip, S. Ding, Lee R. Yeh, and Huay B. Pan

**BACKGROUND AND PURPOSE:** Metabolites in pyogenic brain abscesses, as detected with *in vivo* proton MR spectroscopy, are different from those found in brain and can help differentiate pyogenic brain abscesses from necrotic neoplasms. We compared the findings of *in vivo* with those of *in vitro* MR spectroscopy and categorized the MR spectral patterns with respect to the causative organisms and abscess size.

**METHODS:** Fifteen patients with pyogenic brain abscesses underwent *in vivo* 1.5-T  $^1\text{H}$  MR spectroscopy and had findings of ring enhancement. The causative organisms were determined from cultures of aspirated pus. Single-voxel  $^1\text{H}$  MR spectroscopy was performed with the point-resolved method (1600/270, 135 TR/TE). In six representative patients, *in vitro* 11.7-T  $^1\text{H}$  MR spectra were obtained from the aspirated pus.

**RESULTS:** Three *in vivo* MR spectral patterns were noted: A) presence of lactate at 1.3 ppm, cytosolic amino acids (leucine, isoleucine, and valine) at 0.9 ppm, alanine at 1.50 ppm, and acetate at 1.92 ppm, with the presence or absence of succinate at 2.4 ppm and lipids (0.8–1.3 ppm), representing mostly obligate anaerobes or a mixture of obligate and facultative anaerobes; B) presence of lactate at 1.3 ppm and cytosolic amino acids at 0.9 ppm, with the presence or absence of lipids but not acetate or alanine (0.8–1.3 ppm), representing mostly obligate aerobes or facultative anaerobes; and C) presence of lactate at 1.3 ppm alone, showing small abscess. Additional resonance peaks of lysine at 1.73 and 3.0 ppm, glutamate/glutamine at 2.09–2.36 ppm, taurine at 3.24 and 3.42 ppm, glycine at 3.55 ppm, and amino acids at 3.75 ppm could be observed in the *in vitro* MR spectra.

**CONCLUSION:** Results from the *in vivo* observations were satisfactorily verified by the *in vitro* experiments. The *in vitro* measurements may offer complementary information that cannot be extracted from *in vivo* MR spectra. Determination of the three  $^1\text{H}$  MR spectral patterns may be helpful in devising the best possible treatment plans for patients with pyogenic abscesses.

Brain abscesses are usually diagnosed on the basis of findings from CT and MR imaging, together with the clinical manifestations. Unfortunately, however, the

combination of nonspecific clinical findings and similarities in morphologic appearances often makes it difficult to distinguish abscesses from other brain lesions, especially metastases and glioblastomas. Clinically, both brain abscesses and brain tumors may cause headaches, focal neurologic deficits, epileptic seizures, and disturbances in higher level cortical function. Also, brain abscesses induce fever in only 50% of cases, because the fever may be masked by corticosteroid therapy. Radiologically, a brain abscess in the capsule stage appears on CT and MR images as an expansile, ring-enhancing mass surrounded by edema; this appearance is similar to that of necrotic brain tumors (1, 2).

The ability to make a rapid diagnosis of a brain abscess is very important in order to provide the correct medical treatment. Findings from several studies suggest that *in vivo* proton ( $^1\text{H}$ ) MR spectros-

Received March 22, 2004; accepted after revision May 19.

From the Departments of Radiology (P.H.L., C.C.H., L.R.Y., H.B.P.) and Neurosurgery (S.S.H., C.W.Y.), Veterans General Hospital-Kaohsiung, National Yang-Ming University, Taiwan, and the Department of Chemistry (K.T.L., S.D.), National Sun Yat-Sen University, Taiwan, Republic of China.

Supported by grants from National Science Council NSC-91-2314-B-075B-008 and NSC-92-2314-B-075B-003 (P.H.L.) and NSC-92-2113-M-110-019 (S.D.) and Ministry of Education A-92-N-FA01-2-4-5 (S.D.).

Presented at the 42 annual meeting of the American Society of Neuroradiology, Seattle, WA, June 5–11, 2004.

Address reprint requests to Ping-Hong Lai, MD, Department of Radiology, Veterans General Hospital-Kaohsiung, 386 Ta-Chung First Rd, Kaohsiung, Taiwan 813, Republic of China.

copy might noninvasively contribute to the establishment of the differential diagnosis between brain tumors and abscesses. MR spectra are available for a small number of patients with pyogenic brain abscesses and are considered to be different from those for necrotic tumor (3–14). It has been suggested that  $^1\text{H}$  MR resonances from succinate (2.4 ppm), acetate (1.92 ppm), and alanine (1.5 ppm), as well as from the three amino acids valine, leucine, and isoleucine (0.9 ppm), are potential abscess markers (5, 6, 7–10).

Our study had two objectives. First, we compared *in vivo* with *in vitro* MR spectroscopic findings. Second, we categorized the MR spectral patterns with respect to the causative organisms and abscess size. After the completion of our study, Garg et al (15) reported the results of a similar study, which appeared a few months after the first version of this work was submitted.

## Methods

### Patient Population

From November 2001 to January 2003, 15 patients (10 men and five women; age range, 28–78 years) with pyogenic brain abscesses were included in the study. The pyogenic abscesses were of otogenic origin in five patients, blood-borne in four, and the result of head injury with CSF rhinorrhea in one patient. For the remaining five patients, no focus of infection could be found. The abscesses were located in the frontal lobe ( $n = 3$ ), parietal lobe ( $n = 3$ ), temporal lobe ( $n = 3$ ), occipital lobe ( $n = 2$ ), basal ganglion ( $n = 1$ ), and cerebellum ( $n = 1$ ). The abscesses were multiple in the remaining two patients. Except in one patient (patient 15) with multiple miliary pyogenic abscesses, all the abscesses were larger than  $6\text{ cm}^3$ .

Diagnosis of an abscess was confirmed by aspiration of pus in 14 patients. No aspiration was performed in one patient who responded to medical management and showed complete regression at follow-up examinations. Four patients were treated with open drainage and 10 with repeated needle aspiration, combined with antibiotic treatment in all cases. In 12 of the 14 patients with an abscess, the causative agents were confirmed by the results of cultures of aspirated pus. Four patients had an infection with *Streptococcus intermedius*, one with *Streptococcus constellatus*, one with *Streptococcus mitis* and *Enterococcus faecalis*, one with *Staphylococcus aureus*, one with *Eubacterium lentum*, two with *Pseudomonas aeruginosa*, and two with *Bacteroides fragilis*. In the other two patients, Gram-positive cocci ( $n = 1$ ) or Gram-negative bacilli ( $n = 1$ ) were seen in smears of aspirated pus, but no growth was obtained. There was no clinical or laboratory evidence of infection in six of the 15 patients with brain abscess. Two patients had a history of nasopharyngeal cancer and had received radiation therapy for several years. Twelve patients were cured after surgery and antibiotic treatment, and one patient was cured by antibiotic treatment alone. Two patients died due to complications. The clinical information is summarized in the Table.

### MR Imaging and *In Vivo* $^1\text{H}$ MR Spectroscopy

All MR imaging and *in vivo*  $^1\text{H}$  MR spectroscopy studies were performed with a clinical 1.5-T system (Signa, GE Medical Systems, Milwaukee, WI) with a quadrature head coil. The routine imaging studies included multiplanar T1-weighted spin-echo (500/30/2 [TR/TE/NEX]), T2-weighted fast spin-echo (4000/100/2) with echo train length 8, and fast fluid-attenuated inversion-recovery (9000/133/2200/1 [TR/TE/TI/NEX]) sequences. We used T1-weighted or T2-weighted imaging to locate the voxels for the  $^1\text{H}$  MR spectroscopic

studies. The selection of voxel position in the estimated center of the lesion was determined visually by examining the MR images in three orthogonal planes (sagittal, coronal, and axial) to define a  $2 \times 2 \times 2\text{-cm}$  volume of interest. Contrast-enhanced (Gadolinium-DTPA; Magnevist, Schering AG, Berlin, Germany) T1-weighted images were acquired for all patients.

$^1\text{H}$  MR spectroscopy was applied by using the method of point-resolved spectroscopy. After automated transmitter and receiver adjustment, the signal over the volume of interest was shimmed to within a typical full-width at a half-maximum of 4–8 Hz in all examinations. Optimal water resonance suppression was achieved by preirradiation of the water resonance with three chemical shift selective pulse sequences and spoiled gradient pulses. The parameters used were 1600/270/192 (TR/TE/acquisitions), a spectral width of 2500 Hz, and 2048 data points in all patients. For all patients, additional MR spectra were obtained with a 135-ms TE to confirm the phase inversion associated with J-coupled metabolites of alanine, lactate, and amino acids, but not of lipids, which may be helpful in discriminating lactate or amino acid signals from lipid signals (5, 8). The acquisition time for each sequence was 5 minutes 45 seconds.

The  $^1\text{H}$  MR spectroscopy data files were transferred to an off-line workstation for postprocessing by using a spectroscopy analysis package according to the following steps: DC correction, zero filling to 4096 data points, 1.0-Hz exponential apodization, Fourier transformation, and zero-order phase correction. Assignment of resonance peaks for the metabolites was based on previously documented MR spectroscopic studies of necrotic brain tumors and brain abscesses (3, 5–14). The resonance peaks including lactate at 1.3 ppm, cytosolic amino acids (leucine, isoleucine, and valine) at 0.9 ppm, alanine at 1.50 ppm, acetate at 1.92 ppm, succinate at 2.4 ppm, and lipids (0.8–1.3 ppm) were analyzed in all patients. Resonance peaks were arbitrarily assigned to one of three grades—low (+), medium (++), or high (+++)—relative to the peak height of water. The method by which arbitrary peak grades were assigned has been described in detail elsewhere (8).

### *In Vitro* $^1\text{H}$ MR Spectroscopy

*In vitro* studies were performed on samples from six patients, by using a 500-MHz (11.7-T) nuclear MR spectrometer (Unity Inova; Varian, Palo Alto, CA), to confirm the assignment of resonances observed *in vivo*. The excised or drained pus was immediately frozen in liquid nitrogen; 250  $\mu\text{L}$  of thawed samples were then poured into 5-mm nuclear MR tubes. A capillary tube that contained 3-trimethylsilyl-2,2,3,3-tetradeuteriosodium propionate in deuterium oxide at a concentration of 10 mmol/L was used as an external chemical shift and concentration reference. The sequence parameters for single pulse-collected spectra were as follows: TR, 1200 ms; pulse angle,  $90^\circ$ ; spectral width, 5190 Hz; data points, 5400; number of signal averages, 64. A 1D Hahn spin-echo sequence (11,500/135 [TR/TE]; spectral width, 5190 Hz; data points, 4152; number of signal averages, 64) was also used, to confirm the presence of J-coupled metabolites. Furthermore, these J-couplings can be shown more quantitatively and more specifically with 2D nuclear MR spectroscopy.

In a standard 2D correlation spectroscopy (COSY) spectrum, a diagonal peak corresponds to the signal from the same proton spin while a cross peak corresponds to the presence of J-coupling between two different (normally adjacent, separated by three bonds) proton spins (16). The presence of J-coupling between two adjacent protons is therefore clearly shown in a COSY spectrum as a cross peak between the two resonance frequencies of the coupled protons.

The other advantage of COSY or other 2D or higher-dimensional spectrum is that a higher resolution than that with a 1D spectrum is achieved, so that more quantitative and more specific information on J-coupled spin pairs can be obtained; that is, the coupling between the methyl groups in amino acids (leucine, isoleucine, and valine) can be unambiguously identi-

Clinical information and <sup>1</sup>H MR spectroscopic findings in 15 patients with pyogenic brain abscesses

Patient No./Sex/ Age (y)	Chief Complaint	Location of Abscess	Pus Culture Microorganisms	Treatment	Outcome	Duration of Symptoms	Spectroscopy before/after Starting Antibiotics	MR Spectroscopic Findings									
								Pattern	NAA	Cr	Cho	Succ	Ace	Ala	AA	Lac	Lip
1/F/45	Fever, headache, unstable gait	Left cerebellum	<i>Bacteroides fragilis</i>	Surgery/medical	Cured	10 days	1 day after	A	+	+	++	++	+++	++	++	+++	++
2/M/74	Right hemiparesis	Left parietal	<i>Streptococcus intermedius</i>	Surgery/medical	Cured	30 days	1 day before	A	-	-	-	-	+	+	++	++	-
3/M/69	Fever, right hemiparesis	Left parietal	<i>B fragilis</i>	Surgery/medical	Died	7 days	1 day before	A	+	+	+	++	+++	+	++	++	+
4/M/48	Headache	Left frontal	Negative	Surgery/medical	Cured	10 days	2 days before	A	-	-	-	-	+++	++	+++	+++	+
5/M/45	Fever, headache	Right temporal	<i>Streptococcus mitis</i> , <i>Enterococcus faecalis</i>	Surgery/medical	Cured	12 days	2 days after	A	-	-	-	++	++	+	+++	+++	-
6/M/43	Consciousness change	Right basal ganglion	<i>Eubacterium lentum</i>	Surgery/medical	Cured	3 days	1 day after	A	-	-	-	++	++	++	++	+++	-
7/M/47	Headache, left homonymous hemianopia	Right occipital	<i>S intermedius</i>	Surgery/medical	Cured	14 days	1 day after	B	-	-	-	-	-	-	+	++	-
8/F/28	Right homonymous hemianopia	Left occipital	<i>S intermedius</i>	Surgery/medical	Cured	21 days	2 days before	B	-	-	-	-	-	-	+	++	-
9/M/76	Fever, consciousness change	Left temporal	Negative	Surgery/medical	Cured	14 days	1 day after	B	+	+	+	-	-	-	+	++	-
10/F/69	Left hemiparesis	Right frontal	<i>Staphylococcus aureus</i>	Surgery/medical	Cured	3 days	1 day before	B	+	+	+	-	-	-	+	++	-
11/F/29	Fever, headache	Left frontal	<i>Pseudomonas aeruginosa</i>	Surgery/medical	Cured	2 wks	2 days after	B	-	-	-	-	-	-	+	++	+
12/M/72	Fever, left hemiparesis	Right parietal	<i>S intermedius</i>	Surgery/medical	Cured	10 days	2 days before	B	+	+	+	-	-	-	+	++	-
13/M/72	Left hemiparesis, infective endocarditis	Multiple	<i>Streptococcus constellatus</i>	Surgery/medical	Died	30 days	1 day after	B	-	-	-	-	-	-	+	++	-
14/F/78	Fever, consciousness change	Right temporal	<i>P aeruginosa</i>	Surgery/medical	Cured	10 days	2 days after	B	-	-	-	-	-	-	+	++	-
15/M/72	Consciousness change, infective endocarditis	Multiple military (<5 mm)	<i>S mitis</i> (blood culture)	Medical	Cured	3 days	1 day after	C	++	+	++	-	-	-	-	+	-

Notes.—Negative sign indicates no bacterial growth; +, small peak; ++, moderate peak; +++, large peak; Ace, acetate; Ala, alanine; AA, amino acids; Lac, lactate; Succ, succinate; NAA, N-acetyl/aspartate; Cho, choline; Cr, creatine-phosphocreatine; Lip, lipids.

fied (5, 9, 11). Therefore, both COSY and single 90° spectra were acquired to help discriminate and identify compounds of similar or identical resonance frequencies, with frequency-selective water presaturation. The spectral width was 5300 Hz in both dimensions. The number of data points was 4096 in t2 dimension and 256 in t1 dimension. The number of averages obtained was 48 for each t1 step. The data were filtered with sine-bell windows, zero-filled in both dimensions, and then Fourier transformed. The total acquisition time for each COSY spectrum was about 300 minutes.

## Results

### In Vivo <sup>1</sup>H MR spectroscopy

The clinical characteristics of patients and the *in vivo* <sup>1</sup>H MR spectroscopy findings are summarized in the Table. The MR spectra of all patients were of acceptable quality. The predominant resonance lines, *N*-acetylaspartate (NAA), choline (Cho) and creatine-phosphocreatine (Cr), which are usually observed in the parenchyma of the normal brain, were hardly detectable in the central necrotic fluid of the abscesses. In six patients, 10–20% of the volume of interest contained adjacent normal or edematous brain tissues as estimated from multisection images.

*In vivo* <sup>1</sup>H MR spectroscopy of brain abscess depicted multiple resonance peaks. The amino acids appeared of particular importance among these abscess markers, as amino acids have not been demonstrated by *in vivo* spectroscopy in cystic or solid neoplastic tumors. Discrimination between amino acids (i.e., valine, leucine, and isoleucine at 0.9 ppm) and lipid (at 0.8 to 1.2 ppm) is important, because lipid signals may exist in both brain tumors and abscesses. We used a TE of 135 ms, causing the resonance peaks of the lactate doublet and amino acid multiplets to invert because of J-coupling, whereas resonances from lipids did not invert because of uncoupled spins. We found three different *in vivo* <sup>1</sup>H MR spectral patterns of pyogenic brain abscesses in the 15 patients in this study: pattern A, presence of lactate at 1.3 ppm, cytosolic amino acids (leucine, isoleucine, and valine) at 0.9 ppm, alanine at 1.50 ppm, and acetate at 1.92 ppm, along with the presence or absence of succinate at 2.4 ppm and lipids (0.8–1.3 ppm) (Fig 1); pattern B, presence of lactate at 1.3 ppm and cytosolic amino acids at 0.9 ppm, along with the presence or absence of lipids (0.8–1.3 ppm) (Fig 2); and pattern C, presence of lactate at 1.3 ppm (Fig 3). Patients 1–6 showed spectral pattern A; patients 7–14, pattern B; and patient 15, pattern C.

The bacteriologic data obtained from the pus culture and the spectral pattern of the pus are summarized in the Table. All patients with pattern A received antibiotics for 1–2 days before or after spectroscopic examination. All six patients showed the presence of lactate, cytosolic amino acids, alanine, and acetate. Succinate was observed in four patients, and lipids were observed in three patients. Succinate was always present in conjunction with acetate but never present alone in any of the patients in our study. One patient (patient 4) had no bacterial growth

in the pus culture. The cultures for pattern A mostly showed obligate anaerobes or a mixture of obligate and facultative anaerobes.

All patients with pattern B received antibiotics for 1–2 days before or after spectroscopic examination. All eight patients showed the presence of lactate and cytosolic amino acids. Lipids were observed in one patient. One patient (patient 9) had no bacterial growth in the pus culture. The culture for pattern B mostly showed obligate aerobes or facultative anaerobes.

The patient with pattern C received antibiotics for 1 day before spectroscopic examination and had multiple milary abscesses associated with infective endocarditis and *Streptococcus mitis* bacteremia. This patient showed the presence of lactate. Almost complete remission of the formation of diffuse abscesses after antimicrobial therapy was identified 3 months later (Fig 3D).

### In Vitro <sup>1</sup>H MR Spectroscopy

Six *in vitro* <sup>1</sup>H MR spectroscopic measurements were performed on the aspirated fluid. The 1D <sup>1</sup>H MR spectra from patient 6 are shown in Figure 1D and E, and Figure 1F shows the 2D COSY <sup>1</sup>H MR spectrum obtained from the aspirated pus of patient 6. The 1D <sup>1</sup>H MR spectra from patient 14 are shown in Figure 2D and E, and Figure 2F shows the 2D COSY <sup>1</sup>H MR spectrum obtained from the aspirated pus of patient 14.

Comparison of the *in vivo* and *in vitro* <sup>1</sup>H MR spectra (Figs 1 and 2) permitted the tentative assignment of the <sup>1</sup>H MR resonance lines detected *in vivo* in the brain abscesses. The complex multiplet, centered at 0.9 ppm and inverted in the 135-ms TE spectrum, has been assigned to various amino acids on the 1D spin-echo spectra (Figs 1D and 2D).

Amino acids, lactate (1.3 ppm), and alanine (1.5 ppm) were inverted in the 135-ms TE spectrum (Figs 1E and 2E). The observation of these inverted peaks is clear evidence of the presence of metabolites in the pus samples of the patients, because signal inversion at a TE of about 135 ms corresponds to the J-coupling value of about 7 Hz. These J-couplings were more clearly shown in 2D COSY spectra by the observation and assignment of the relevant cross peaks.

The 2D COSY spectra suggest that these amino acids are mainly valine ( $\delta_1$ ;  $\delta_2$  = 1.02; 2.28), leucine ( $\delta_1$ ;  $\delta_2$  = 0.96; 1.72), and isoleucine ( $\delta_1$ ;  $\delta_2$  = 0.96; 1.99) (Figs 1F and 2F). The resonance line at 1.92 ppm was assigned to acetate and the 2.4 ppm resonance line was assigned to succinate. Both resonance lines were detected in the <sup>1</sup>H MR spectra obtained from Figure 1, and not observed in the spectra from Figure 2.

Several additional resonance lines could be assigned in the *in vitro* <sup>1</sup>H MR spectra. In the 1D <sup>1</sup>H MR spectra, the following were found: a multiplet centered at 1.73 and 3.0 ppm and presumably due to lysine and to unidentified macromolecules; a complex



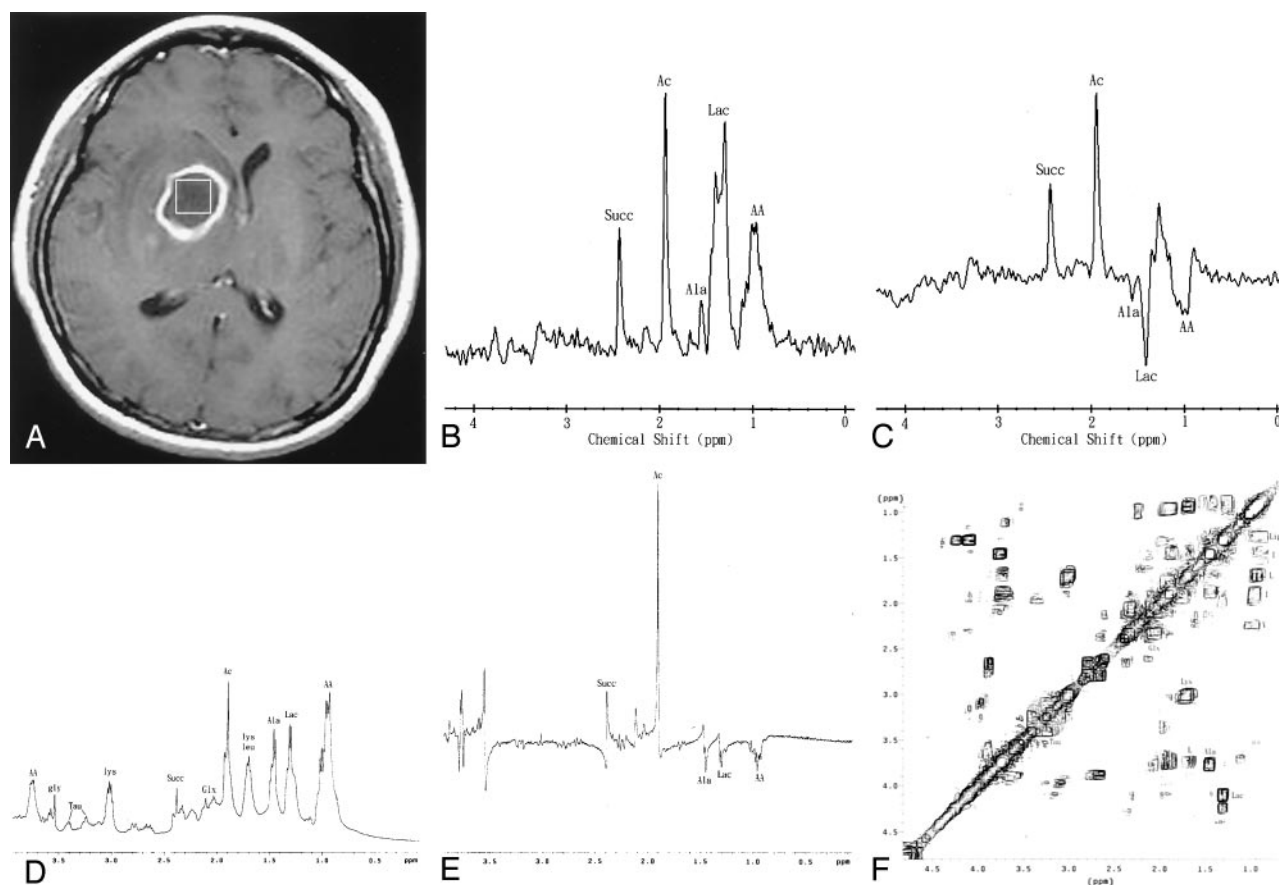


FIG 1. Patient 6. A 43-year-old man with surgically proved pyogenic brain abscess in the right basal ganglion secondary to *Eubacterium lentum* (obligate anaerobe) infection.

A, Axial contrast-enhanced T1-weighted MR image (500/30) shows a ring-shaped cystic lesion and surrounding edema. The 2 x 2 x 2-cm voxel (box) in the center of the lesion represents the  $^1\text{H}$  MR spectroscopic volume of interest.

B and C, *In vivo*  $^1\text{H}$  MR spectra (TR/TE 1600/270 [B] and 1600/135 [C]) from the abscess cavity show spectral pattern A, which represents succinate (Succ), acetate (Ac), alanine (Ala), lactate (Lac), and amino acids (AA). At a TE of 135 ms (C), the phase reversal resonances are well depicted at 1.5, 1.3, and 0.9 ppm, which confirms the assignment to alanine, lactate, and amino acids, respectively.

D and E, One-dimensional, *in vitro*, single-pulse (D) and spin-echo (TE = 135 ms; E) spectra of the pus removed from the abscess cavity show the prominent resonance for acetate (Ac), as well as signals for succinate (Succ), alanine (Ala), lactate (Lac), amino acids (AA) at 0.9 and 3.75 ppm, leucine (Leu), lysine (Lys) at 1.73 and 3.0 ppm, glutamate/glutamine (Glx) at 2.09–2.36 ppm, glycine (Gly) at 3.55 ppm, and taurine (Tau) at 3.24 and 3.42 ppm. Alanine is equally prominent as lactate *in vitro*, compared with the *in vivo* study. Note the phase reversal at 1.5, 1.3, and 0.9 ppm, suggesting alanine, lactate, and amino acids, respectively, in the spin-echo (135 ms) spectrum (E).

F, *In vitro* 2D COSY spectrum of the pus obtained from the abscess cavity assigns leucine (L), isoleucine (I), valine (V), lipids (Lip), and lysine (Lys) unambiguously. COSY spectrum shows the J-couplings between amino acids and other metabolites, as well as the difference between the coupling values of amino acids and other metabolites. The individual amino acids (e.g., leucine, isoleucine, and valine) can be identified only through 2D COSY. Ala indicates alanine; Glx, glutamate/glutamine; Lac, lactate; Tau, Taurine.

multiplet at 2.09–2.36 ppm and assigned to glutamate/glutamine; a triplet centered at 3.24 and 3.42 ppm and assigned to taurine; a singlet centered at 3.55 ppm and assigned to glycine; a complex multiplet centered at 3.75 ppm and likely due to amino acids. On the 1D spin-echo MR spectra with the TE of 135 ms, peaks of amino acids (i.e., valine, isoleucine, and leucine), lactate, and alanine showed almost complete inversion of phase, whereas the signals of the rest of the metabolites (lysine, glutamate/glutamine, taurine, glycine) were virtually unchanged. This means the J-couplings observed in amino acids are significantly different from those in other metabolites. This difference was also shown in the 2D COSY spectra: the cross peaks from valine, leucine, isoleucine, lactate,

alanine, and lysine were normally fairly off-diagonal, whereas the cross peaks from the glutamate/glutamine, taurine, and lipids were close to diagonal (Fig 1F).

## Discussion

Diffusion-weighted (DW) imaging and  $^1\text{H}$  MR spectroscopy are valuable in the differential diagnosis of abscesses and cystic necrotic tumors (3–14). Hyperintensity with restricted diffusion is diagnostic of, but not pathognomonic for, pyogenic abscess on DW images. The cystic or necrotic portions of the tumors almost always have a low signal intensity on DW

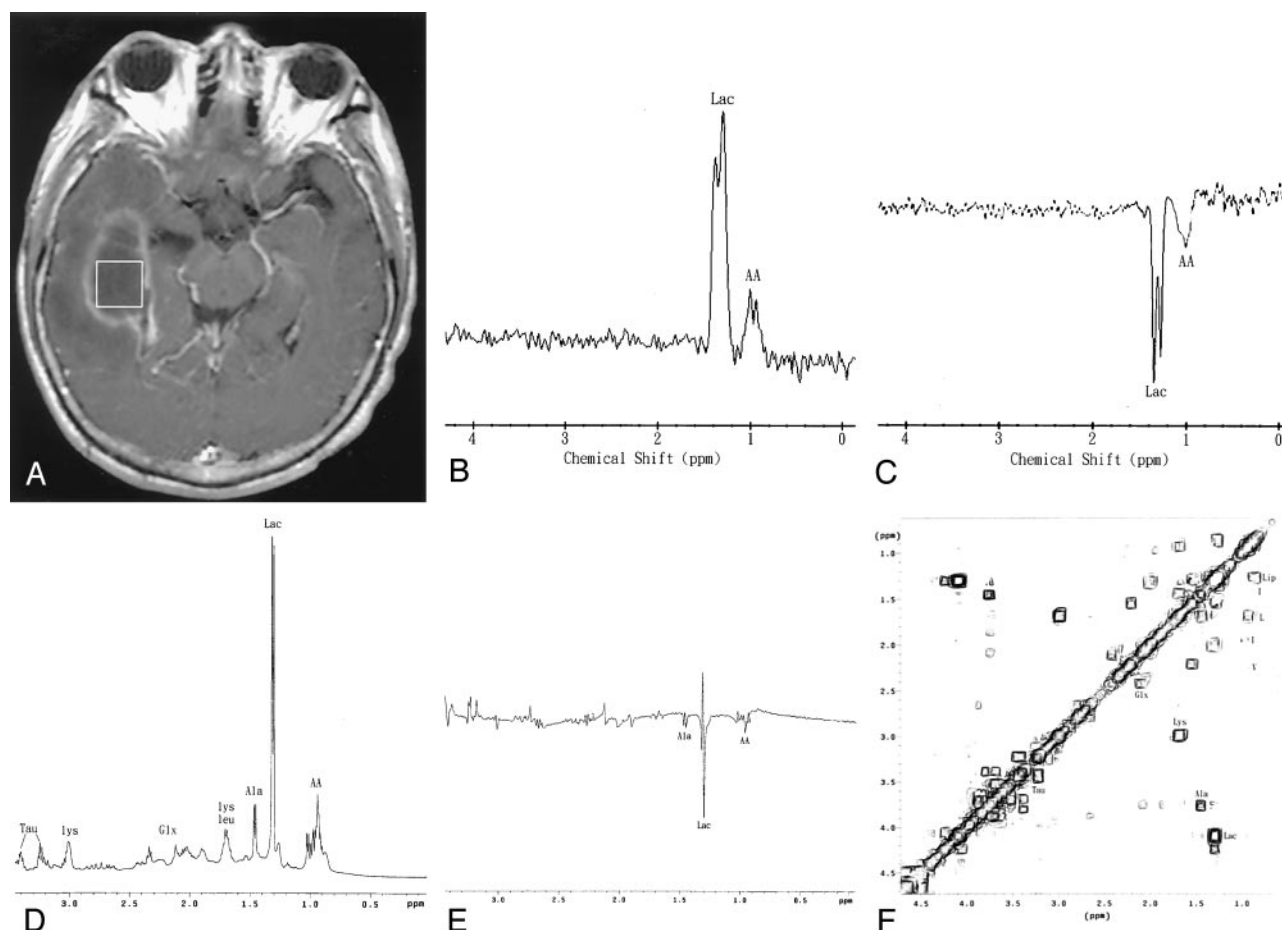


FIG 2. Patient 14. A 78-year-old woman with surgically proved pyogenic brain abscess and ventriculitis in the right temporal region secondary to *Pseudomonas aeruginosa* (aerobe) infection.

A, Axial contrast-enhanced T1-weighted MR image (500/30) shows a regular thin-walled ring-enhanced cystic lesion and adjacent temporal horn ventricular enhancement and surrounding edema. The 2 x 2 x 2-cm voxel (box) in the center of the lesion represents the  $^1\text{H}$  MR spectroscopic volume of interest.

B and C, *In vivo*  $^1\text{H}$  spectra (TR/TE 1600/270 [B] and 1600/135 [C]) from the abscess cavity show spectral pattern B with only two resonance peaks identified; however, the phase reversal of the amino acid (AA) signal at 0.9 ppm is depicted on the MR spectrum obtained with a 135-msec TE (C), which is indicative of a pyogenic brain abscess. Lac indicates lactate.

D and E, One-dimensional, *in vitro*, single-pulse (D) and spin-echo (TE = 135 ms; E) spectra of the pus removed from the abscess cavity show the signals for lactate (Lac), amino acids (AA), alanine (Ala), glutamate/glutamine (Glx), leucine (Leu), and lysine (Lys). Alanine is present and more prominent *in vitro*, compared with the *in vivo* study. Note the phase reversal at 1.5, 1.3, and 0.9 ppm, suggesting alanine, lactate, and amino acids, respectively, in the spin-echo (135 ms) spectrum.

F, *In vitro* 2D COSY spectrum of the pus obtained from the abscess cavity assigns leucine (L), isoleucine (I), valine (V), lipids (Lip), and lysine (Lys) unambiguously. The individual amino acids (e.g., leucine, isoleucine, and valine) can be identified only through 2D COSY. Ala indicates alanine; Glx, glutamate/glutamine; Lip, lipid; Lys, lysine; Tau, Taurine.

images and a higher apparent diffusion coefficient value; however, some exceptions have been reported for necrotic brain tumors (17, 18). Single-voxel  $^1\text{H}$  MR spectroscopy is also useful in differentiating ring-like enhanced lesions that cannot be diagnosed correctly by using contrast-enhanced MR imaging alone (6–8, 10, 12, 14), but MR spectroscopy may be more limited in the cases of smaller peripheral lesions and skull base lesions (14). Several reports have indicated the significance of MR spectral metabolites in pyogenic brain abscesses (3–14). According to our objectives, discussion of the contents of pyogenic brain abscesses is divided into two parts: part 1, *in vivo* versus *in vitro* MR spectroscopic findings, and part 2, MR spectroscopy and bacteriologic comparison.

### In Vivo versus In Vitro MR spectroscopic Findings

In brain abscess spectra, there are usually no detectable resonances originating from the usual major brain and tumor metabolites (NAA, Cr, and Cho) except a partial volume of the adjacent normal or edematous brain tissues. The *in vivo*  $^1\text{H}$  MR spectral pattern A of the abscess cavity, illustrated by the case of patient 6 (Fig 1), showed the presence of acetate (1.92 ppm), succinate (2.4 ppm), and some amino acids (0.9 ppm), as well as lactate (1.3 ppm), and corresponded with findings at *in vitro* MR spectroscopy (Fig 1). The *in vivo*  $^1\text{H}$  MR spectral pattern B of our study showed the presence of lactate at 1.3 ppm and amino acids at 0.9 ppm, without obvious peaks

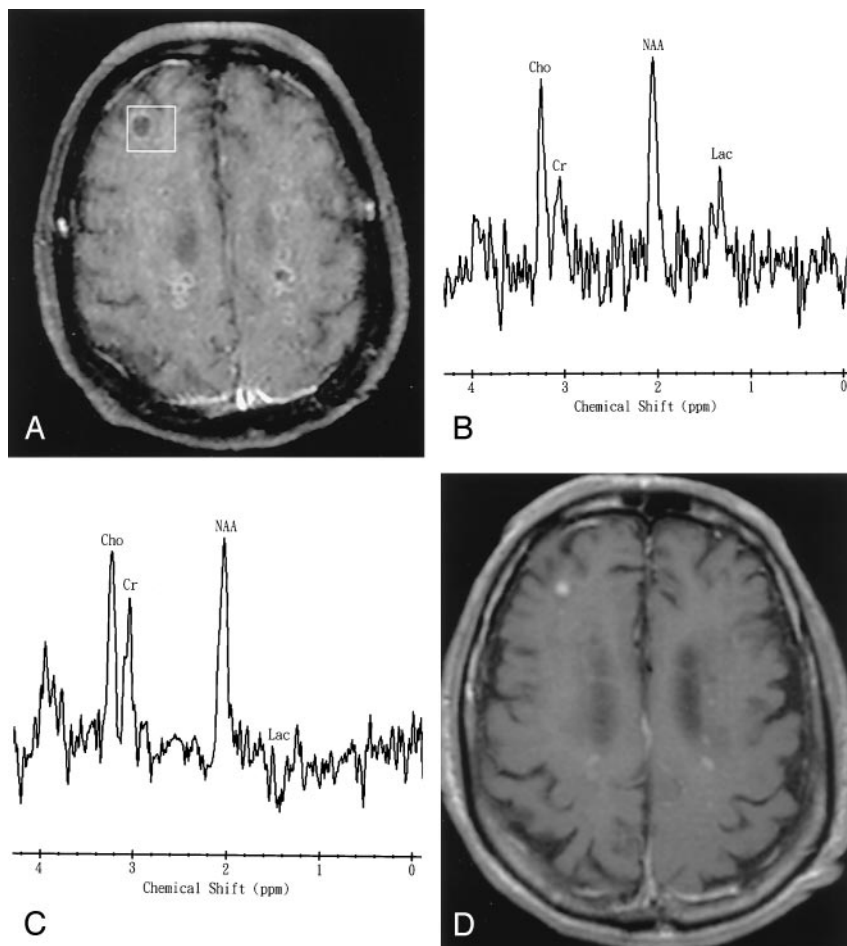


FIG 3. Patient 15. A 72-year-old man with *Streptococcus mitis* (aerobe) bacteremia, infective endocarditis, and multiple miliary pyogenic brain abscesses.

A, Axial contrast-enhanced T1-weighted MR image shows numerous miliary nodules with ring enhancement. The 2 x 2 x 2-cm voxel (box) in the lesion and adjacent brain tissue represents the  $^1\text{H}$  MR spectroscopic volume of interest.

B and C, *In vivo*  $^1\text{H}$  spectra (TR/TE 1600/270 [B] and 1600/135 [C]) show spectral pattern C with a lactate (Lac) peak (1.3 ppm) that is inverted at a TE of 135. The resonances of choline (Cho), creatine (Cr), and N-acetylaspartate (NAA) were interpreted to be caused by partial volume effects of the adjacent brain tissue. The phase reversal does not follow the classic pattern in this case because of the presence of some phase distortion, which presumably originated from the eddy current effect. Multiple small peaks at various frequencies are present; these peaks may represent noise or unassigned metabolites.

D, Axial contrast-enhanced T1-weighted MR image obtained 3 months later shows almost complete remission of the formation of diffuse abscesses after antibiotics.

attributed to acetate (1.92 ppm) and succinate (2.4 ppm). We confirmed the *in vivo* spectral assignment by performing *in vitro* 1D and 2D COSY  $^1\text{H}$  MR spectroscopy (Fig 2).

Compared with the *in vivo* spectra, a number of additional resonance peaks of the lysine at 1.73 and 3.0 ppm, of the glutamate/glutamine at 2.09–2.36 ppm, of the taurine at 3.24 and 3.42 ppm, of glycine at 3.55 ppm, and of amino acids at 3.75 ppm could be observed on the 1D single-pulse or spin-echo spectrum, or in the 2D COSY  $^1\text{H}$  MR spectra. The fact that the signals of glycine and amino acids were not detected *in vivo* may be attributed to two major reasons: first, the much lower detection sensitivity in the downfield region of the spectrum for the digital filter used, and second, the effect of insufficient water signal suppression (5). Failure to detect signals from lysine, taurine, and other metabolites *in vivo* can be explained by the low concentration of these compounds in tissue, more complex coupling patterns *in vivo* than *in vitro*, or shorter proton transverse relaxation times in tissue (5, 9). The detection of these additional signals from *in vitro* measurement signifies the importance of *in vitro* experiments, because supplementary information may be obtained to complement that extracted from *in vivo* experiments.

### MR Spectroscopy and Bacteriologic Comparison

Abscess formation has been divided into four stages on the basis of histopathologic data: early cerebritis, followed by infiltration by inflammatory and macrophage cells, enlargement of necrosis, and capsule formation (19). The central necrotic fluid abscess contains necrotic brain tissue, bacteria, and acute inflammatory cells, such as polymorphonucleocytes. Necrosis of the cell membrane results in the release of free fatty acids and proteins. Lactate (1.3 ppm) and lipids (0.8–1.3 ppm) are nonspecific metabolites resulting from glycolysis and necrotic brain tissue in the brain abscess. Both lactate and lipid peaks can also be observed in the necrotic tumor (5, 6, 8–11).

Increases in lactate, acetate, and succinate presumably originate from the enhanced glycolysis and fermentation of the infecting microorganisms (5–12). Bacteria differ in their possession of the four major glycolytic pathways: Embden-Meyerhof-Parnas, hexose monophosphate, Entner-Doudoroff, and phosphoketolase (20, 21). The Embden-Meyerhof-Parnas pathway is found in almost all bacteria, whether aerobic or anaerobic bacteria. Pyogenic bacteria ferment glucose via the glycolytic pathway and produce a large pool of pyruvate. Energy generation in bacteria depends on glycolysis and fermentation under anaerobic



conditions. The start-up point of fermentation is pyruvate and the major fermentation pathways include lactic, alcoholic, mixed acid, propionic, and butanediol fermentation (20, 21).

Lactate is produced by various fermentative pathways, such as homolactic or heterolactic fermentation, which are carried out by all members of the *Streptococcus*, *Pediococcus*, and *Lactobacillus* genera. These fermentation pathways may be the main source of lactate in the abscess cavity. Acetate can be produced during heterolactic fermentation, propionic acid fermentation, and mixed acid fermentation in many *Lactobacillus* species, many *Propionibacterium* species, and in most of the Enterobacteriaceae (20, 22). Acetate could be a key marker of infection. Succinate is known to be one of the end products of propionic acid fermentation and mixed acid fermentation in various anaerobic bacteria (3, 5, 23). Among these, succinate is known to be a marker of anaerobic bacterial infection (19). Acetate and succinate seem to be characteristic of pyogenic brain abscesses, especially in those due to obligate anaerobes or a mixture of obligate and facultative anaerobes, confirmed as shown by the pattern A spectrum (Fig 1). These findings are similar to those of group 1 in the recent report by Garg et al (15). The spectral pattern can be explained by the evidence that the pyruvate may go after the anaerobic fermentation path of pyruvate by anaerobes, where it may undergo carboxylation to form succinate via oxaloacetate, malate, and fumarate; and a portion of the pyruvate may also form acetate (15, 20, 21).

The detection of these end products is often applied in identifying the various bacterial strains present in abscesses. This is usually done by means of gas-liquid chromatography, either from culture media following isolation of the bacteria (24, 25) or from the pus sample itself (23, 26). There are limitations to the direct extrapolation of *in vitro* pus analysis data (26).

In the present study, *Streptococcus intermedius* was found in the bacterial culture from four patients (patients 2, 7, 8, and 12). Spectra in three of these patients showed resonance peaks attributed to lactate and amino acids, and the spectra in one patient showed peaks attributed to lactate, acetate, and amino acids. The fact that acetate was not detected in the  $^1\text{H}$  MR spectra from most of the above patients may reflect the low concentration in the pus of the bacteria generating these end products and/or different bacterial strains in the pus (5).

The *in vivo*  $^1\text{H}$  MR spectroscopic pattern B with aerobes and facultative anaerobes shows the absence of acetate and succinate (Fig 2). These findings are similar to those of group 2 in the recent report by Garg et al (15). Pattern B can be explained by the evidence that the pyruvate from glycolysis may enter into the citric acid cycle in aerobes and in facultative anaerobes in the presence of oxygen. Although succinate is one of the intermediate metabolites of the citric acid cycle, succinate does not store up during its formation and quickly transforms to the next inter-

mediate compound (27). This event results in the absence of succinate in the pattern B spectra.

We had two sterile culture cases; one case was a pattern A (lactate, amino acids, acetate, with or without succinate) and the other case was a pattern B (lactate and amino acids). Garg et al (15) reported that sterile cultures were characterized as lactate and amino acids (like pattern B in our study). The differences in the results of these two studies possibly may be due to multiple factors, such as inadequate sampling, or specimen transport preventing recovery of anaerobes present, or undergoing extended antibiotic treatment (15, 28).

With *in vivo*  $^1\text{H}$  MR spectroscopy, we observed high levels of various amino acids in brain abscesses. These amino acids are a result of the breakdown of proteins by proteolytic enzymes after phagocytosis and autolysis mediated by polymorphonucleocytes in pus (5–12). These amino acids are seen in both patterns A and B spectra. It is also important to emphasize that the detection of amino acids in brain abscesses applies only to bacterial infections (12). In cases of nonbacterial abscesses, such as one hydatid cyst reported by Kohli et al (29), two tuberculomas reported by Kaminogo et al (30), and 11 toxoplasmic abscesses and four cryptococcomas reported by Chang et al (31), no amino acids were detected.

The *in vivo*  $^1\text{H}$  MR spectroscopic pattern C revealed the presence of lactate at 1.3 ppm. The patient had multiple miliary abscesses and received antibiotics for 1 day before the spectroscopic examination. The Cho, Cr, and NAA peaks were caused by partial volume effects of the adjacent brain tissue, and only a lactate peak was found in the single-voxel spectrum of this patient (Fig 3).

Single-voxel  $^1\text{H}$  MR spectroscopy is limited in voxel size from  $1.5 \times 1.5 \times 1.5$  cm to  $2 \times 2 \times 2$  cm clinically, and smaller lesions are more affected by the partial volume effect in  $^1\text{H}$  MR spectroscopy. An amino acid peak was not detected in this single-voxel spectrum, possibly owing to this effect and a low concentration in the pus. The finding of this nonspecific spectrum in the case of small abscesses should be borne in mind to avoid incorrect diagnosis. We should be careful in the interpretation of this nonspecific spectrum due to a small abscess, because it results in the pitfall of the MR spectra in the diagnosis of the abscess. Chemical shift imaging may have a smaller voxel than the single-voxel technique in the case of small lesions.

The pattern C spectrum has also been mentioned in treated abscesses (11, 13, 14). Dev et al (11) demonstrated a decline in acetate and pyruvate in five patients after 1 week of aspiration and medical treatment. The authors believe that the disappearance of metabolites of bacterial origin suggests a positive response to therapy. Burtscher and Holtas (13) showed a dramatic change in the follow-up MR spectroscopy of abscesses occurring 29 and 113 days after beginning antibiotic treatment. All resonances (representing succinate, acetate, alanine, and amino acids) except that of lactate disappeared. Thus, spectral

specificity may be valid only for untreated abscesses or abscesses at the start of treatment (11, 13, 14).

In general, empiric therapy of a brain abscess depends on the origin of infection. Surgical stereotactic aspiration or excision is the reference standard for the therapy. Empiric antibiotic coverage can be modified on the basis of results of Gram stain and culture of pus obtained from the abscess. All patients should receive a minimum of 6–8 weeks of parenteral antibiotic therapy (27). In certain situations, however, surgery is not recommended, and antibiotic therapy may be the only alternative. Such situations could include a deep-seated abscess or an abscess in a critical area not amenable to a safe surgical approach and patients who are poor surgical candidates (e.g., those with poorly controlled bleeding) (32).

According to the results of bacteriologic information and the MR spectral patterns in our study, the optimal treatment plans for brain abscess may be as follows: For pattern A, most causative organisms are obligate anaerobes or such facultative anaerobes as *Streptococcus intermedius* and *Streptococcus mitis*, which are universally susceptible to penicillin and/or metronidazole (32). Accordingly, such patients without obvious mass effect could receive antibiotics alone. Serial CT or MR imaging should be performed on a weekly basis to closely follow up the changes in the abscess. Surgical intervention should be performed whenever deterioration of neurologic status or enlargement of the abscess is seen. For patterns B and C, the microbial causes are diverse, so the appropriate empiric antibiotic therapy is limited. Therefore, we recommend early surgical drainage of the abscess and antimicrobial therapy based on the results of Gram stain and culture of the pus aspirated from the abscess.

### Conclusion

Three different spectral patterns were seen in pyogenic brain abscesses with *in vivo*  $^1\text{H}$  MR spectroscopy. The spectral metabolite pattern A of lactate, amino acids, alanine, and acetate, with or without succinate, shows an abscess caused by obligate anaerobes or a mixture of obligate and facultative anaerobes. The spectral metabolite pattern B of lactate and amino acids reveals an abscess caused by obligate aerobes or facultative anaerobes. The spectral pattern C of lactate alone shows small and/or treated abscesses. This information may be helpful in designing treatment plans for patients with brain abscesses. The results from the *in vivo* observations were well verified by the results of the *in vitro* experiments. It is also significant that the *in vitro* measurements may offer complementary information that cannot be extracted from *in vivo* MR spectra.

### Acknowledgment

The authors thank Hsiao-Wen Chung, PhD, for helpful comments on MR spectroscopy and Dr. Shue-Ren Wann for invaluable advice on preparing the manuscript.

### References

1. Lau DW, Klein NC, Cunha BA. **Brain abscess mimicking brain tumor.** *Heart Lung* 1989;18:634–637
2. Mamelak AN, Mampalam TJ, Obana WG, Rosenblum ML. **Improved management of multiple brain abscesses: a combined surgical and medical approach.** *Neurosurgery* 1995;36:76–85
3. Demaerel P, Van Hecke P, Van Oostende S, et al. **Bacterial metabolism shown by magnetic resonance spectroscopy.** *Lancet* 1994;344:1234–1235
4. Harada M, Tanouchi M, Miyoshi H, Nishitani H, Kannuki S. **Brain abscess observed by localized proton magnetic resonance spectroscopy.** *Magn Reson Imaging* 1994;12:1269–1274
5. Rémy C, Grand S, Lai ES, et al.  **$^1\text{H}$  MRS of human brain abscess in vivo and in vitro.** *Magn Reson Med* 1995;34:508–514
6. Poptani H, Gupta RK, Jain VK, Roy R, Pandey R. **Cystic intracranial mass lesions: possible role of in vivo MR spectroscopy in its differential diagnosis.** *Magn Reson Imaging* 1995;13:1019–1029
7. Grand S, Lai ES, Esteve F, et al. **In vivo  $^1\text{H}$  MRS of brain abscesses versus necrotic brain tumors.** *Neurology* 1996;47:846–848
8. Kim SH, Chang KH, Song IC, et al. **Brain abscess and brain tumor: discrimination with in vivo  $^1\text{H}$  MR spectroscopy.** *Radiology* 1997;204:239–245
9. Martinez-Perez I, Moreno A, Alonso J, et al. **Diagnosis of brain abscess by magnetic resonance spectroscopy.** *J Neurosurg* 1997;86:708–713
10. Chang KH, Song IC, Kim SH, et al. **In vivo single voxel proton MR spectroscopy in intracranial cystic masses.** *AJNR Am J Neuroradiol* 1998;19:401–405
11. Dev R, Gupta RK, Poptani H, Roy R, Sharma S, Husain M. **Role of in vivo proton magnetic resonance spectroscopy in the diagnosis and management of brain abscesses.** *Neurosurgery* 1998;42:37–43
12. Grand S, Passaro G, Ziegler A, et al. **Necrotic tumor versus brain abscess: importance of amino acids detected at  $^1\text{H}$  MR spectroscopy: initial results.** *Radiology* 1999;213:785–793
13. Burtcher IM, Holtas S. **In vivo proton MR spectroscopy of untreated and treated brain abscesses.** *AJNR Am J Neuroradiol* 1999;20:1049–1053
14. Lai PH, Ho JT, Chen WL, et al. **Brain abscess and necrotic brain tumor: discrimination with proton MR spectroscopy and diffusion-weighted imaging.** *AJNR Am J Neuroradiol* 2002;23:1369–1377
15. Garg M, Gupta RK, Husain N, et al. **Brain abscesses: etiologic categorization with in vivo proton MR spectroscopy.** *Radiology* 2004;230:519–527
16. Ernst RR, Bodenhausen G, Wokaun A. **Two-dimensional correlation methods based on coherence transfer.** In: Ernst RR, Bodenhausen G, Wokaun A, eds. *Principles of Nuclear Magnetic Resonance in One and Two Dimensions*. Oxford, England: Clarendon Press, 1987:400–489
17. Park SH, Chang KH, Song IC, Kim YJ, Kim SH, Han MH. **Diffusion-weighted MRI in cystic or necrotic intracranial lesions.** *Neuroradiology* 2000;42:716–721
18. Holtas S, Geijer B, Stromblad LG, Maly-Sundgren P, Burtcher IM. **A ring-enhancing metastasis with central high signal on diffusion-weighted imaging and low apparent diffusion coefficients.** *Neuroradiology* 2000;42:824–827
19. Britt RH, Engmann DR, Yeager AS. **Neuropathological and computerized tomographic findings in experimental brain abscess.** *J Neurosurg* 1981;55:590–603
20. Willett HP. **Energy metabolism.** In: Joklik WK, Willett HP, Amos DB, Wilfert CM, eds. *Zinsser Microbiology*, 19th ed. Stamford, CT: Appleton Lange, 1988:25–43
21. Jurtshuk P. **Bacterial metabolism.** In: Baron S, ed. *Medical Microbiology*, 2nd ed. Galveston, TX: University of Texas, 1996:65–84
22. Stryer L. **Generation and storage of metabolic energy.** In: Stryer L, ed. *Biochemistry*, 2nd ed. San Francisco, CA: Freeman, 1981:233–283
23. Gorbach SL, Mayhew JW, Bartlett JG, Thadepalli H, Onderdonk AB. **Rapid diagnosis of anaerobic infections by direct gas-liquid chromatography of clinical specimens.** *J Clin Invest* 1976;57:478–484
24. Holdeman LV, Cato EP, Moore WEC. *Anaerobe Laboratory Manual*. Blacksburg, VA: Virginia Polytechnic Institute and State University Anaerobe Laboratory, 1977
25. Deacon AG, Duerden BI, Holbrook WP. **Gas-liquid chromatography**

- graphic analysis of metabolic products in the identification of **Bacteroidaceae of clinical interest**. *J Med Microbiol* 1978;11:81-99
26. Phillips KD, Tearle PV, Willis AT. Rapid diagnosis of anaerobic infections by gas-liquid chromatography of clinical material. *J Clin Pathol* 1976;29:428-432
27. Stryer L. **Citric acid cycle**. In: Stryer L, eds. *Biochemistry*, 4th ed. New York: Freeman, 1998:509-528
28. Hill GB. **Introduction to the anaerobic bacteria: non-spore forming anaerobes**. In: Joklik WK, ed. *Zinsser Microbiology*, 18th ed. East Norwalk, CT: Appleton-Century-Crofts, 1984:679-695
29. Kohli A, Gupta RK, Poptani H, Roy R. **In vivo proton magnetic resonance spectroscopy in a case of intracranial hydatid cyst**. *Neurology* 1995;45:562-564
30. Kaminogo M, Ishimaru H, Morikawa M, Suzuki Y, Shibata S. **Proton MR spectroscopy and diffusion-weighted MR imaging for the diagnosis of intracranial tuberculomas: report of two cases**. *Neurol Res* 2002;24:537-543
31. Chang L, Miller BL, McBride D, et al. **Brain lesions in patients with AIDS: <sup>1</sup>H MR spectroscopy**. *Radiology* 1995;197:525-531
32. Fischer SA, Harris AA. **Bacterial abscess**. In: Gorbach SL, Bartlett JG, Blacklow NR, eds. *Infectious Diseases*, 2nd ed. Philadelphia: W.B. Saunders, 1998:1431-1444